Docking and Molecular Dynamics Study on the Inhibitory Activity of Coumarins on Aldose Reductase

Zhiguo Wang,[†] Baoping Ling,[‡] Rui Zhang,[†] and Yongjun Liu*[,†,‡]

Northwest Institute of Plateau Biology, Chinese Academy of Sciences, Xining, Qinghai 810001, China, and School of Chemistry and Chemical Engineering, Shandong University, Jinan, Shandong 250100, China

Received: April 16, 2008

In order to explore the inhibitory mechanism of coumarins toward aldose reductase (ALR2), AutoDock and Gromacs software were used for docking and molecular dynamics studies on 14 coumarins (CM) and ALR2 protease. The docking results indicate that residues TYR48, HIS110, and TRP111construct the active pocket of ALR2 and, besides van der Waals and hydrophobic interaction, CM mainly interact with ALR2 by forming hydrogen bonds to cause inhibitory behavior. Except for CM1, all the other coumarins take the lactone part as acceptor to build up the hydrogen bond network with active-pocket residues. Unlike CM3, which has two comparable binding modes with ALR2, most coumarins only have one dominant orientation in their binding sites. The molecular dynamics calculation, based on the docking results, implies that the orientations of CM in the active pocket show different stabilities. Orientation of CM1 and CM3a take an unstable binding mode with ALR2; their conformations and RMSDs relative to ALR2 change a lot with the dynamic process. While the remaining CM are always hydrogen-bonded with residues TYR48 and HIS110 through the carbonyl O atom of the lactone group during the whole process, they retain the original binding mode and gradually reach dynamic equilibrium.

1. Introduction

Despite recent advances in the chemistry and molecular pharmacology of antidiabetic drugs, diabetes still remains a life-threatening disease to human beings, and syndromes caused by diabetes bring great physical and psychological suffering to patients. It is estimated that diabetes will be one of the world's most common diseases and biggest public health problems within a few decades.[1] Several experiments have revealed a correlation between glucose metabolism via the polyol pathway (see Figure 1) and long-term diabetic complications. Aldose reductase (alditol/$NADP^+$ oxidoreductase, EC 1.1.1.21, ALR2), the first enzyme found in the pathway, is a key rate-limiting protease which catalyzes the NADPH-dependent reduction of glucose to sorbitol.[2,3] Under normal circumstances, the ALR2 affinity with glucose is low, and has a weak activity. In a hyperglycemic environment, ALR2 is highly activated, resulting in the increase of glucose metabolism rate by 2−4 times; meanwhile, sorbitol-dehydrogenase dependent sorbitol has a common metabolism rate and poor penetration through cellular membranes. This can lead to severe accumulation of sorbitol, hyperosmotic stress, cellular swelling, perturbation of the membrane transport process under hyperglycemic conditions, and finally initiation of cellular lesions associated with late-onset diabetic complications such as neuropathy, nephropathy, retinopathy, cataracts, and cardiovascular disease.[3–5] As the activation of ALR2 has been considered to be a very important factor in the onset of diabetes syndrome, aldose reductase inhibitors (ARIs) have received much attention as an attractive strategy to prevent or delay the onset and to minimize the seriousness of chronic diabetic complications.

According to structural characteristics, currently known ARIs can be divided into three classes: (I) carboxylic acids, including Alrestatin, Tolrestat, Zopolrestat, and Epalrestat; (II) cyclic imides, such as Sorbinil and Fidarestat; (III) flavonoids, a series of compounds mainly from natural sources whose prototype is Quercetin[6] (see Figure 2). In vitro, carboxylic acids and cyclic imides exhibit similar inhibitory activity. However, in vivo, the latter is more active because of its poor tissue penetration of carboxylic acids, which is inherent to the conspicuous difference between their pK_a values (3−4) and blood pH (∼7.4).[7–9] Although the spiroimide Sorbinil is highly ALR2-inhibitive and can significantly improve diabetic peripheral neuropathy, its low selectivity of ALR2 from the aldo−keto protease family can cause a serious hypersensitivity reaction; hence the research on Sorbinil has been terminated.[9] Flavonoids widely exist in natural products, and the high ALR2 inhibitory activity as well as inherent antioxidant activity makes them some of the most promising drug candidates.[10–12] Although much progress has been made in the study of ARIs, current inhibitors are still not satisfactory, especially in the selectivity and side effects. Research on new ARIs is still the focus of attention.

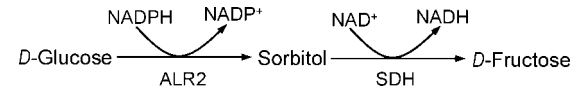

Figure 1. Polyol pathway of D-glucose metabolization.

Coumarins (CM) are a sort of lactone compound with bicyclic structures (Figure 2); their richest sources are plants of *Rutaceae* and *Umbelliferae*.[13] Some of the isolated coumarins show interesting biological activities. For example, Decursin from *Angelica gigas* presents toxic activity against various human cancer cell lines,[14,15] while Soulattrolide from *Calophylum teysmanii* is a potent inhibitor of HIV-I reverse transcriptase.[16] Coumarins have a rigid main structure similar to that of flavonoids (Figure 2), and their inhibitory effects on ALR2 have also been reported. In 1974, Mishkinsky[17] experimentally

[†] Chinese Academy of Sciences.
[‡] Shandong University.

10.1021/jp8033227 CCC: $40.75
Published on Web 07/19/2008

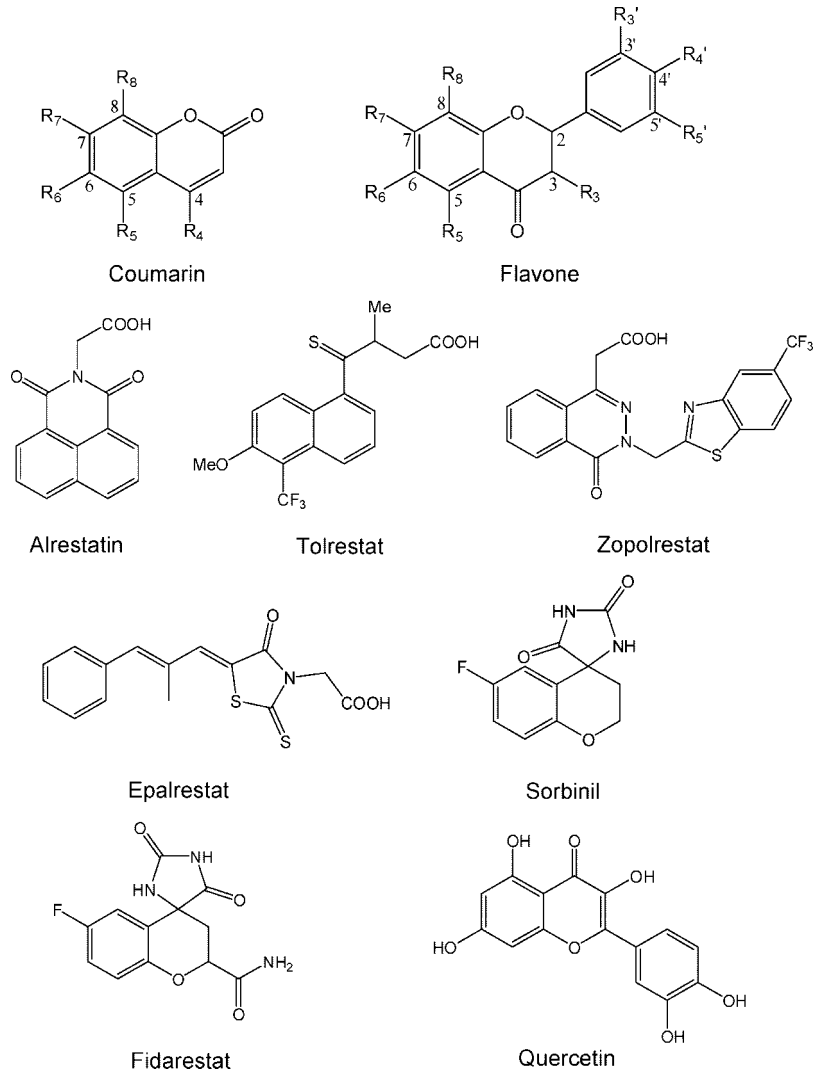

Figure 2. Structures of coumarin and flavone together with some orally active ALR2 inhibitors.

studied the effect of extracts of *Semen Trigonellae* and *Lupinus termis* on rat glucose, alkaloid and coumarins were considered to play an important role in the decrease of glucose; Okuda[18] investigated the inhibition of flavones, flavonoids, and coumarins on rat and bovine aldose reductase; Abram[19] tested a series of synthesized coumarin compounds by using rat lens ALR2. They found the molecules with carboxylic groups showed the strongest inhibition. Although some progress has been made in experimental research, theoretical studies on the inhibition of coumarins toward ALR2 are still rare. Up to now, only Amic[20] studied the structure−activity relationship of coumarins by using an ordered orthogonalized multivariate linear regression method. They found that the substitution of the original hydroxyl and carboxyl by methyl would greatly decrease the inhibition activity.

Although these studies may provide us some information on the correlation of CM structure and its inhibition activity, the binding mode of CM and ALR2, the binding energy, and the dynamic stability are still unknown. Therefore, in this paper, we made a molecular docking and dynamics study to locate the binding site, get their dynamics information, and further understand the inhibition mechanism of CM toward ALR2.

2. Methods

2.1. Preparation of Substrate/Enzyme Model. ***Substrate Preparation.*** Currently there are still no extensive experimental studies on coumarin ALR2 inhibitors, so we mainly selected 14 CM molecules which bear structure diversity from refs 20 and 21. In order to explore the influence of different substituents on binding conformations and inhibitory activities, the quantum Gaussian 03[22] package was used to get the most stable CM conformations. The structure-optimizing calculation was carried out at the 6-31(d) level by employing the Becke three-parameter Lee−Yang−Parr hybrid density functional theory, and the structures with the lowest energy were selected for the following docking study. When docking, the Gasteiger−Marsili atomic charge was chosen; it is also the selection of AutoDock while calculating the empirical free energy function.[23,24]

Enzyme Preparation. The crystal structure of human ALR2 complexed with Tolrestat and cofactor $NADP^+$ from Brookhaven Protein Data Bank (PDB ID code: 2FZD) was used in the docking experiments.[24] Crystallographic waters which were not hydrogen-bonded to the enzyme were deleted and the complex was energy minimized by a 500-step conjugate gradient. Then, the whole protein was minimized by constraining the position of the backbone atoms. During this step, $NADP^+$ was allowed to move. Energy minimizations were realized by setting a 10

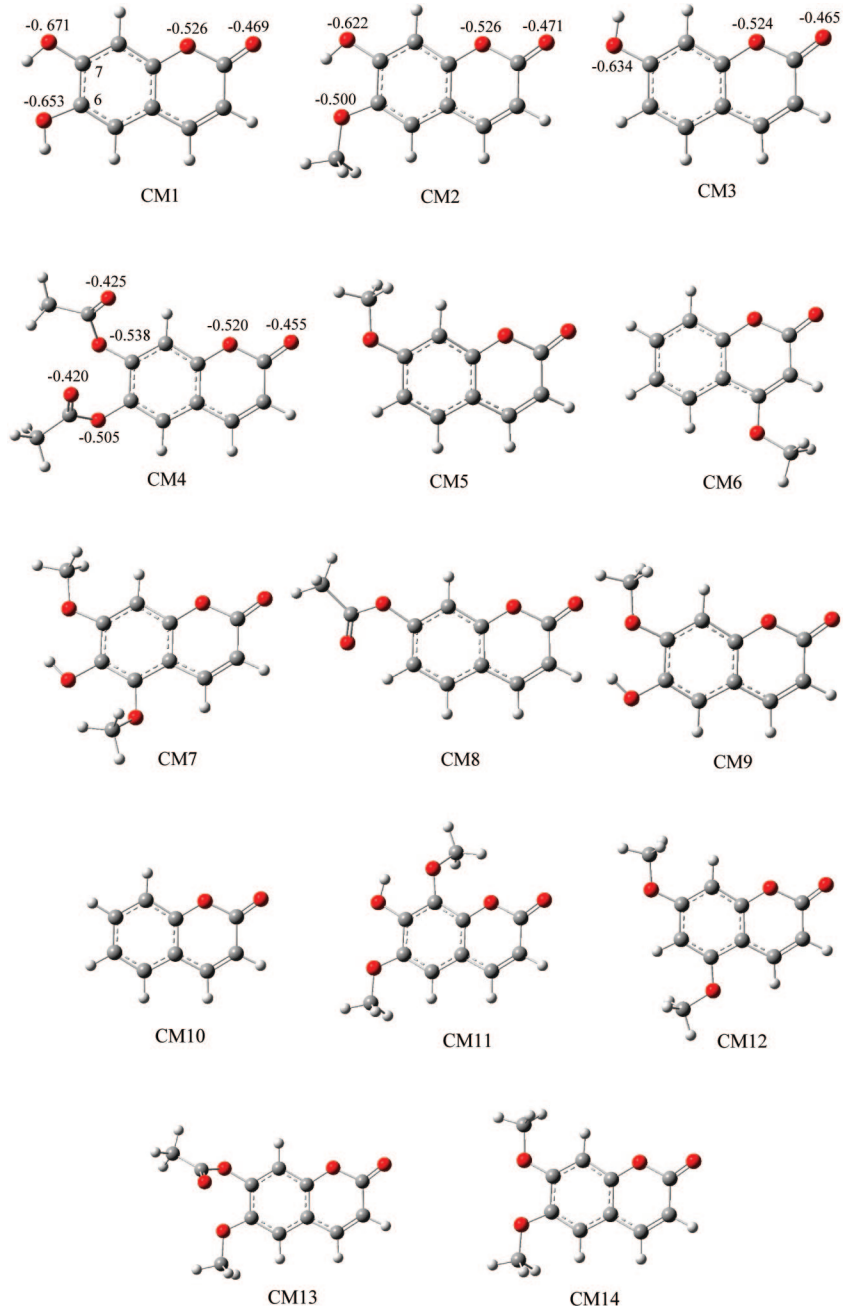

Figure 3. Structures of coumarin derivatives optimized by Gaussian 03 package at B3LYP/6-31G(d) level.

Å nonbonded cutoff and an 0.01 kcal/mol energy gradient convergence criterion. So far, all these steps were done by using the Gromacs force field. Finally, the Tolrestat was deleted, and the remaining complex was used as the starting structure in the docking study.

Although the inhibition assays of our compounds were conducted on bovine lens ALR2, the use of a model of human ALR2 for docking studies is justified by the following fact: the crystal structure of bovine ALR2 is still unknown, but all the active-site residues including those of the specialty pocket are largely conserved across the ALR2 isoforms so far sequenced.[25]

2.2. Parameter Setting for Docking and Gromacs Dynamics Calculation. ***AutoDock Setup.*** Docking was performed with version 4.0 of the program AutoDock,[26] which combines a rapid energy evaluation through precalculated grids of affinity potentials with a variety of search algorithms to find suitable binding positions for a ligand on a given protein. When docking, ALR2 was kept rigid, but all the torsional bonds in CM were set free to perform flexible docking. Polar hydrogens were added by using the Hydrogens module in AutoDock Tools (ADT) for ALR2; after that, Kollman united atom partial charges were assigned.[24]

Docking of CM to ALR2 was carried out using the empirical free energy function and the Lamarckian genetic algorithm, applying a standard protocol with an initial population of 150 randomly placed individuals, a maximum number of 2.5×10^7 energy evaluations, a mutation rate of 0.02, a crossover rate of 0.80, and an elitism value of 1, where the average of the worst energy was calculated over a window of the previous 10 generations. For the local search, the so-called Solis and Wets algorithm was applied, using a maximum of 300 iterations. The probability of performing a local search on an individual in the population was 0.06, and the maximum number of consecutive successes or failures before doubling or halving the local search

step size was 4. Fifty independent docking runs were carried out for each ligand. Results were clustered according to the 1.0 Å root-mean-square deviation (RMSD) criterion. All torsion angles for each compound were considered flexible. The grid maps representing the proteins in the actual docking process were calculated with AutoGrid. The grids (one for each atom type in the ligand plus one for electrostatic interactions) were chosen to be sufficiently large to include not only the active site but also significant portions of the surrounding surface. The dimensions of the grids were thus 60 Å × 60 Å × 60 Å, with a spacing of 0.375 Å between the grid points.

Gromacs Dynamics Setup. Based on the docking results, molecular dynamics (MD) simulations of the CM/ALR2/$NADP^+$ systems were carried out with the Gromacs 3.3.1-1 suite of programs using the Gromacs force field. Each of the complexes was placed in the center of a 72 Å × 72 Å × 72 Å cubic box and solvated by SPC/E water molecules.[27] Na^+ counterions were added to satisfy the electroneutrality condition.

Using the leapfrog algorithm in the NPT ensemble, each component, CM, ALR2, $NADP^+$, H_2O, and Na^+, was separately coupled. The Berendsen temperature coupling and Berendsen pressure coupling (the coupling constants were both set to 0.1) were used to keep the system in a stable environment (300 K, 1 bar). All of the complexes were first energy minimized with the steepest descent method; then a 20 ps position restraining simulation was carried out restraining the ALR2 by a 1000 kJ/mol·Å^2 harmonic constraint to relieve close contacts before the actual simulation; finally, a 3 ns MD simulation was performed. During these steps, the particle mesh Ewald (PME) method for long-range electrostatics, a 10 Å cutoff for van der Waals interactions, a 9 Å cutoff for Coulomb interaction, and the LINCS algorithm[28] for bond constraints were used.

3. Results and Discussion

3.1. Docking. Kador et al.[29] have shown that the structural requirements for ALR2 inhibitory activity consist of a generally planar structure with one or two hydrophobic (aromatic) regions and a polar region which is susceptible to charge-transfer interactions. Both characteristics can be found on some oral inhibitors such as Torestat and Alrestatin (Figure 2). For CM (Figure 3), the main aromatic bicyclic structure provides the hydrophobic group, and the lactone group or some substituents with great polarity provide the negative charge center. All these characters make CM good candidates for ARIs.

The 50 docking conformations for each CM molecule were divided into groups according to a 1.0 Å RMSD criterion by using the Clusterings module in ADT. The groups indicate that, except for CM3 which has two energy-close (less than 0.01 kcal/mol) conformations CM3a and CM3b with almost the same proportion, all the other coumarins mainly take one binding conformation (over 80%). Besides RMSD clustering, AutoDock also uses binding free energy evaluation to find the best binding mode. Energy items calculated by AutoDock include intermolecular energy (constituted by van der Waals energy, hydrogen bonding energy, desolvation energy, and electrostatic energy), internal energy, and torsional energy. The first two items build up docking energy; the first and the third item compose the binding energy. During all these interactions, the hydrogen bond between ligand and enzyme is the most important, because in most cases it can decide the binding strength and the location of ligand, whereas the hydrophobic interaction of some certain groups can affect the inhibition specialty to a large extent.[12,25] The energy information is listed in Table 1, and the interaction modes of CM and ALR2 are shown in Figure 4, where only the amino acids located within 5 Å of the inhibitor are displayed. For a better understanding on the docking conformation differences between CM, a superposition is also given in Figure 5.

TABLE 1: Binding and Docking Energies of Coumarins and ALR2 Calculated by AutoDock

coumarin	binding energy, kcal/mol	docking energy, kcal/mol	inhibition constant (298.15 K), μM	inhibition percentage, %
CM1	−6.28	−6.89	9.75	87
CM2	−6.27	−7.17	11.08	60
CM3a	−6.13	−6.11	32.26	54
CM3b	−6.12	−6.10	32.74	54
CM4	−7.66	−9.37	1.70	14
CM5	−6.59	−6.71	14.85	15
CM6	−6.18	−6.51	29.58	43
CM7	−6.54	−7.89	7.67	29
CM8	−7.33	−8.06	4.03	0
CM9	−6.53	−7.40	7.20	19
CM10	−6.15	−6.15	30.86	11
CM11	−5.95	−7.39	20.75	18
CM12	−6.44	−7.12	18.89	42
CM13	−7.32	−8.54	4.15	11
CM14	−6.55	−7.34	14.79	19

According to the difference between groups used to form hydrogen bonds with ALR2, the CM conformations can be divided into two classes: (I) conformations with hydrogen bonds located on 6,7-substituents, such as CM1; (II) conformations that use the lactone group as a hydrogen bond acceptor. All CM except for CM1 take this binding mode. However, the molecule orientation is not consistent with the hydrogen binding mode. CM1 and CM3a are orientation-close, and far from the hydrophobic residues; all the other conformations are orientated similarly to another direction and immerged in a hydrophobic cavity made up of TRP20, TRP79, TRP219, and LEU300.

The binding mode of CM1 with ALR2 is shown in Figure 4A. It can be seen that CM1 is anchored into the so-called anionic binding site via a network of hydrogen bonds involving TYR48, HIS110, and cofactor $NADP^+$, i.e., the O atom in the 7-hydroxyl forms a 2.25 Å hydrogen bond with a polar H atom of TYR48 and a 1.67 Å one with HIS110. At the same time, the polar H atoms of the 6,7-hydroxyls connect with the carbonyl O atom from $NADP^+$ (NAP313) through hydrogen bonds, with bond lengths of 2.21 and 2.10 Å, respectively. There are two electronegative centers in CM1 labeled with Mulliken charge according to Gaussian 03 calculation (see Figure 3), which locate at the 6,7-hydroxyl and lactone areas. However, AutoDock only gives one dominant binding mode with the 6,7-hydroxyls hydrogen bonded. This can be ascribed to two reasons: first, compared to the lactone area, 6,7-hydroxyls with more negative charge have a stronger electrostatic interaction with the neighboring polar residues, and phenolic hydroxyl is much more prone to electron transfer; second, with their own polar hydrogens, 6,7-hydroxyls can be both hydrogen bond donor and acceptor and provide more hydrogen bonds. These two aspects make hydroxyl excel at both the strength and number of hydrogen bonds, so there is only one optimal binding conformation.

Many similarities of CM1 and flavonoids can be found when binding to ALR2. Costantino et al. have shown that, with the most stable binding mode, flavonoids form hydrogen bonds through the 7-hydroxyl O atom with TYR48 and HIS110. This also explains why the 7-hydroxyl is necessary for flavonoid inhibitors.[9,20] As a matter of fact, at a given dose, CM1 is of the highest activity (87% inhibition), which is close to some

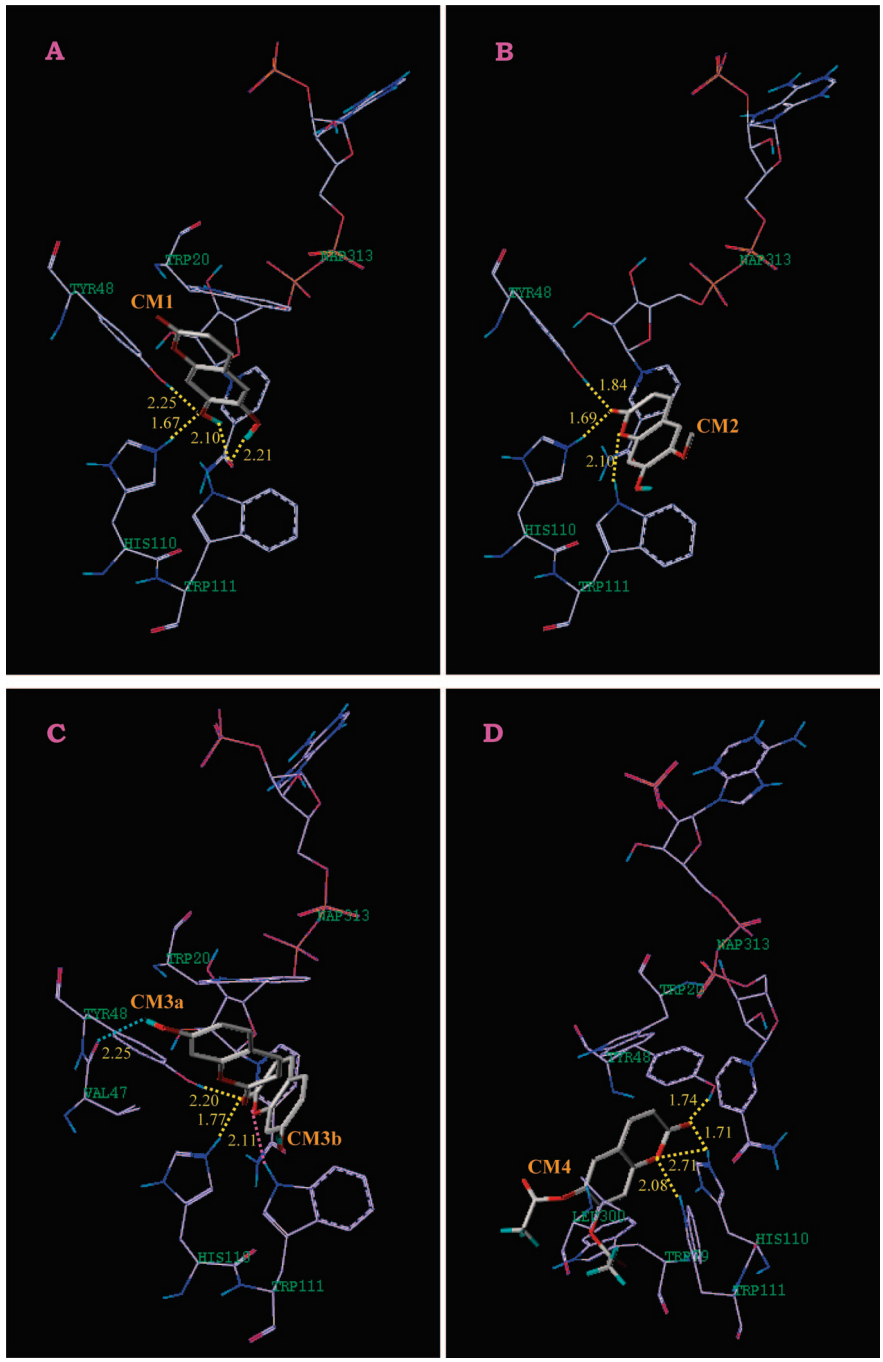

Figure 4. Conformations of coumarin−ALR2 complexes derived by automated docking computation. (A) CM1, (B) CM2, (C) CM3, and (D) CM4. In (C), the yellow dotted lines are used to represent shared hydrogen bond of CM3a and CM3b, the cyan dotted line is for CM3a, and the red dotted line is for CM3b.

flavonoid inhibitors.[20] Another point which should be noted is the orientation of CM1's aromatic ring. Experiments have revealed that the inhibitory selectivity will be completely lost if these flavonoid molecules lose the 2-benzyl group. The docking study proves that the 2-benzyl is buried in a hydrophobic cavity constituted of TRP111 and LEU300.[9] For our docking result, though, the lactone group orients to the polar residue VAL47 and TYR48, the aromatic ring is far from the hydrophobic pocket, which greatly decreases the binding stability. See details under Molecular Dynamics.

Figure 4B gives the binding conformation of CM2. There are also two negative charge centers in CM2, the 6-methoxyl-7-hydroxyl area and the lactone area, and the former is even more charged (Figure 3). However, different from CM1, CM2 surprisingly uses its double-bonded lactone O atom to form hydrogen bonds with TYR48 and HIS110, with bond lengths 1.84 and 1.69 Å, respectively, and the other lactone O atom connects with TRP111 through a 2.10 Å hydrogen bond. The reason for this is that the steric effect and hydrophobic property of the methyl substituent on the 6-methoxyl make CM2 conflict with the polar active-pocket residues, which makes the 6-methoxyl-7-hydroxyl anchored binding mode impossible. On the whole, the hydrogen bond number decreases; however, their bond strength increases judging by the bond length, and CM2 exerts a 60% ALR2 inhibition at the same dose (Table 1).

By structural comparison with CM1, we can find that the methylation of 6-hydroxyl directly changed the binding mode of CM2. This change is of great importance, because it can

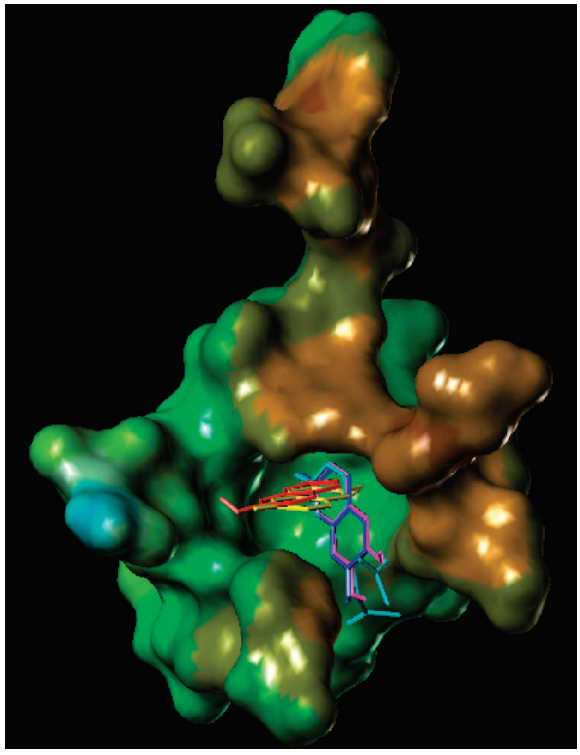

Figure 5. Superposition of structures of CM1, CM2, CM3a, CM3b, and CM4 in the lipophilic potential surface constructed by all the residues that surround the inhibitors within 6.0 Å. As the color changes from brown to green, the surface becomes hydrophilic from hydrophobic gradually. For the sake of distinguishing, yellow is for CM1, magenta for CM2, red for CM3a, blue for CM3b, and cyan for CM4.

make all CM molecules form hydrogen bonds with ALR2 using the lactone group, and ultimately eliminate the pK_a influence by taking no phenolic hydroxyl or carboxyl substituents, which provides us with a good chance to develop a series of novel ARIs. Actually, except for CM1, all the other 13 coumarins are lactone anchored.

From Figure 4C, we can find that CM3 has two binding conformations: CM3a and CM3b have their lactone carbonyl O atoms superposed and, between the molecular planes, an dihedral angle of about 70° exists, which makes their orientations totally different (Figure 5). In the 50 docking conformations, each of them takes an equivalent proportion, and as mentioned above, both are hydrogen-bonded with ALR2 through the lactone group, which takes advantage of negative charge density (Figure 3). In both conformations, the superposed carbonyl O atom is hydrogen-bonded with TYR48 and HIS110, with bond lengths of 2.20 and 1.77 Å (yellow dotted lines). In the meantime, CM3a forms a hydrogen bond with residue VAL47 by its 7-hydroxyl polar H atom (cyan dotted line), while for CM3b another hydrogen bond happens at the other lactone O atom and residue TRP111 (red dotted line). Although differences exist in the orientation and binding modes, CM3a and CM3b have equal numbers of hydrogen bonds which have similar bond strengths. Hence, they have almost the same binding energy and docking energy (Table 1).

In Figure 4D, just like CM2, CM4 takes the same binding conformation: using the lactone group to form a network of hydrogen bonds with TYR48, HIS110, and TRP111, because of the apparent steric hindrance of 6,7-substituents. A minor difference is that there is an additional weak hydrogen bond with a bond length of 2.71 Å between the saturated lactone O atom and residue HIS110; the reason for this is the slight orientation change of body cycle caused by the interaction of 6,7-substituents and LEU300. For the other CM molecules, our docking calculation reveals that they take the same hydrogen bonding mode and molecular orientation as CM2 and CM4.

Comparing binding and docking energies to the inhibition effect in Table 1, we found no good correlation between them. The one that has the highest binding or docking energy does not exhibit the best inhibition, and vice versa. The possible reasons are as follows: (I) when taking the same binding mode, substituents of CM vary a lot in the number of atoms, atom types, and bond torsional freedoms. This is the key factor leading to the energy difference. For example, the 6,7-ethyl carboxylate substituted CM4 has a 1.10 kcal/mol torsional energy, which is much bigger than that of CM2 (about 0.25 kcal/mol). (II) Human ALR2 crystal structure is used instead of the bovine lens aldose reductase; the sequence difference of some amino acids may result in the deviation of the experiment result. (III) Besides binding energy, some other factors can also affect the inhibition ability such as molecular orbital interaction of ligand and acceptor.

3.2. Molecular Dynamics. Based on the docking results, molecular dynamics study of selected bonded complexes (CM1−ALR2, CM2−ALR2, CM3a−ALR2, CM3b−ALR2, and CM4−ALR2) is performed by using the Gromacs program. First, we examined the stability of ALR2 by a 3 ns MD simulation and a following RMSD calculation. Results show that ALR2 becomes equilibrated at 1 ns and afterward. Then the RMSDs of CM to ALR2 were obtained based on the MD simulation of all above five systems to get information on positional fluctuations; see Figure 6. By comparing the RMSD property and conformational changes during simulation, we classified the MD results as (a) CM1−ALR2 and CM3a−ALR2 and (b) CM2−ALR2, CM3b−ALR2, and CM4−ALR2. This is just the same as the classification of binding orientation.

From Figure 6A, it can be seen that CM1 seems "stabilized" relative to ALR2 at 1.3 ns judging by its RMSD deviation. However, by checking the interval conformations, we note that the binding site of CM1 has already changed. By 1.3 ns, the conformation has changed to flat from vertical in Figure 6A. All the original hydrogen bonds have vanished and are substituted by new ones which locate at the carbonyl O atom with LYS21 and the 7-hydroxyl O atom with TRP111. When reaching 2.8 ns, the hydrogen bond of CM1 and TRP111 has also disappeared, and further calculation reveals that, at 3.5 ns, the only connection of CM1 and ALR2 is the hydrogen bond between the carbonyl O atom and residue LYS21 with the CM1 backbone far from the active pocket. Possible reasons for the binding instability are the following. On one hand, the hydrogen bonds located at the 6,7-hydroxyls and $NADP^+$ are not strong enough; on the other hand, the molecular orientation makes the aromatic backbone close to polar residues (such as TYR48) while far from the hydrophobic specialty pocket. The hydrophobic and polar interactions are the driving force to push CM1 from its original binding site.

For CM3a, although taking a different hydrogen binding mode compared to CM1, it is still dynamically unfavorable for the same reason as CM1. Figure 6C gives its RMSD, which shows significant fluctuations. Especially between 0.5 and 1.2 ns, the values are totally off the baseline even up to 0.75 nm. Accordingly, the CM3a molecule is almost entirely out of the active pocket, leaving only the carbonyl O atom hydrogen bonded with TYR48. However, after 1.2 ns, CM3a seems to gradually stabilize and finally reaches equilibrium. As a matter of fact, because the polarity of new neighboring residues make

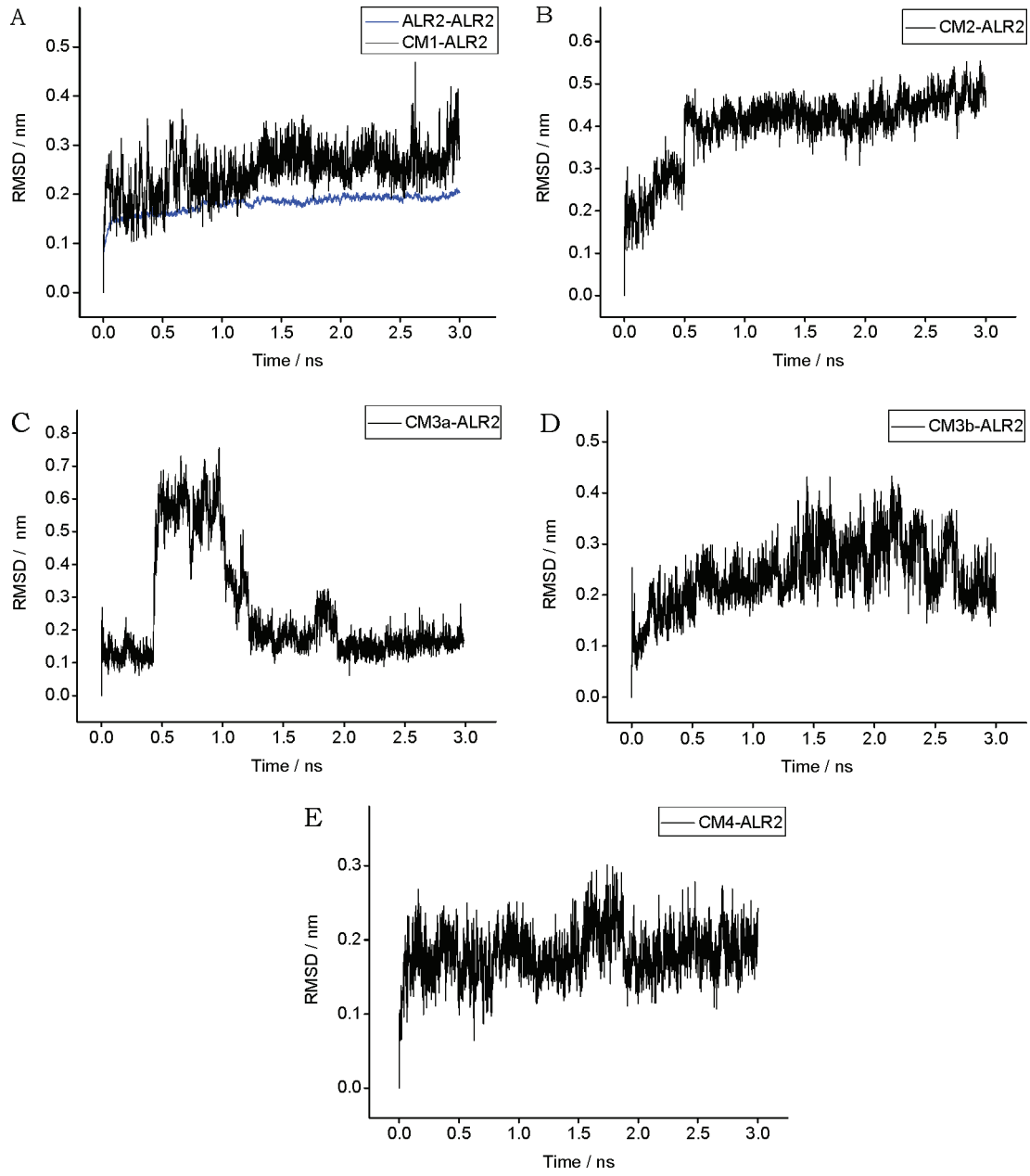

Figure 6. RMSDs of coumarins to ALR2 derived by molecular dynamics calculation using Gromacs software. The RMSD of ALR2 is also presented in (A).

CM3a incompatible with the surroundings, it was been pulled back to the active site again by that hydrogen bond. Also, the average conformation of the last 1.0 ns takes the original hydrogen binding mode, but the aromatic backbone is buried in the hydrophobic pocket, which is particularly like CM3b.

Parts B, D, and E of Figure 6 give the RMSDs of CM2, CM3b, and CM4, which are all relative to ALR2. Compared to CM3a, these graphs seem much more smooth, because their similarly oriented aromatic backbones are all buried in the hydrophobic specialty pocket and belong to the same binding mode. By checking interval and average conformations, we notice that during the whole dynamic process these molecules always hydrogen bond with TYR48 and HIS110 through their carbonyl O atoms, and their equilibrium comes at about 0.8 ns, which is much earlier than CM3a. In summary, coumarins with this kind of orientation can steadily bind with the ALR2 active pocket and have great potential to be good ARIs.

Our dynamics study shows that coumarins can steadily anchor to ALR2 to exert an inhibition effect. Compared to flavonoids, to which the 6,7-hydroxyl substituents are essential, coumarins mainly use the more favorable lactone group, which can provide enough hydrogen bond strength and proper orientation to bind with ALR2.

4. Conclusion

Based on experimental data, molecular docking and dynamics study were performed to explore the inhibition mechanism of coumarins toward ALR2. Our results suggested that CM can exactly bond to the active pocket of ALR2 to display inhibition; the binding mode may alter with the changing of some substituents on certain positions. Only with both 6,7-hydroxyls substituted such as in CM1, can a CM molecule bind to ALR2 with a hydroxyl group. In other cases, coumarins are lactone anchored to the active pocket. The ligand orientation in the active site can greatly affect the stability of the ligand−acceptor complex; moreover, only conformations with CM aromatic backbone buried in the hydrophobic specialty pocket are dynamically stable.

With proper modification, the lactone binding mode can completely eliminate the pK_a effect of carboxyl or hydroxyl groups, and coumarins could be a new kind of promising ARIs.

References and Notes

(1) Diamond, J. *Nature* **2003**, *423*, 599.
(2) Tomlinson, D. R.; Stevens, E. J.; Diemel, L. T. *Trends Pharmacol. Sci.* **1994**, *15*, 293.
(3) Kador, P. F. *Med. Res. Rev.* **1988**, *8*, 325.
(4) Yabe-Nishimura, C. *Pharmacol. Rev.* **1998**, *50*, 21.
(5) Brownlee, M. *Nature* **2001**, *414*, 813.
(6) Sarges, R.; Oates, P. J. *Prog. Drug Res.* **1993**, *40*, 99.
(7) Mylari, B. L.; Armento, S. J.; Beebe, D. A.; Conn, E. L.; Coutcher, J. B.; Dina, M. S.; O'Gorman, M. T.; Linhares, M. C.; Martin, W. H.; Oates, P. J.; Tess, D. A.; Withbroe, G. J.; Zembrowski, W. J. *J. Med. Chem.* **2005**, *48*, 6326.
(8) Eggler, J. F.; Larson, E. R.; Lipinski, C. A.; Mylari, B. L.; Urban, F. J. In *Advances in Medicinal Chemistry*; Maryanoff, E., Maryanoff, C. A., Eds.; Jai Press Inc.: London, 1993; Vol. 2, p 197.
(9) Costantino, L.; Rastelli, G.; Vescovini, K.; Cignarella, G.; Vianello, P.; Del Corso, A.; Cappiello, M.; Mura, U.; Barlocco, D. *J. Med. Chem.* **1996**, *39*, 4396.
(10) Ng, T. B.; Liu, F.; Wang, Z. T. *Life Sci.* **2000**, *66*, 709.
(11) Hans, L.; Winter, D.; Itzstein, M. V. *Biochemistry* **1995**, *34*, 8299.
(12) Maccari, R.; Ottanà, R.; Ciurleo, R.; Vigorita, M. G.; Rakowitz, D.; Steindl, T.; Langer, T. *Bioorg. Med. Chem. Lett.* **2007**, *17*, 3886.
(13) Esténven-Braun, A.; González, A. G. *Nat. Prod. Rep.* **1997**, *14*, 465.
(14) Yim, D.; Singh, R. P.; Agarwal, C.; Lee, S.; Chi, H.; Agarwal, R. *Cancer Res.* **2005**, *65*, 1035.
(15) Song, G. Y.; Lee, J. H.; Cho, M.; Park, B. S.; Kim, D. E.; Oh, S. *Mol. Pharmacol.* **2007**, *72*, 1599.
(16) Hotta, N. *Biomed. Pharmacother.* **1995**, *49*, 232.
(17) Mishkinsky, J. S.; Goldschmied, A.; Joseph, B.; Ahronson, Z.; Sulman, F. G. *Arch. Int. Pharmacodyn. Ther.* **1974**, *210*, 27.
(18) Okuda, J.; Miwa, I.; Inagaki, K.; Horie, T.; Nakayama, M. *Biochem. Pharmacol.* **1982**, *31*, 3807.
(19) Brubaker, A. N.; Ruiter, J. D.; Whitmer, W. L. *J. Med. Chem.* **1986**, *29*, 1094.
(20) Amic, D.; Davidovic-Amic, D.; Beslo, D.; Lucic, B.; Trinajstic, N. *J. Chem. Inf. Comput. Sci.* **1997**, *37*, 581.
(21) Okada, Y.; Miyauchi, N.; Suzuki, K.; Kobayashi, T.; Tsutsui, C.; Mayuzumi, K.; Sansei, N.; Nishibe, S.; Okuyama, T. *Chem. Pharm. Bull.* **1995**, *43*, 1385.
(22) Frisch, M. J.; Trucks, G. W.; Schlegel, H. B.; Scuseria, G. E.; Robb, M. A.; Cheeseman, J. R.; Montgomery, J. A., Jr.; Vreven, T.; Kudin, K. N.; Burant, J. C.; Millam, J. M.; Iyengar, S. S.; Tomasi, J.; Barone, V.; Mennucci, B.; Cossi, M. ; Scalmani, G.; Rega, N.; Petersson, G. A.; Nakatsuji, H.; Hada, M.; Ehara, M.; Toyota, K.; Fukuda, R.; Hasegawa, J.; Ishida, M.; Nakajima, T.; Honda, Y.; Kitao, O.; Nakai, H.; Klene, M.; Li, X.; Knox, J. E.; Hratchian, H. P.; Cross, J. B.; Adamo, C.; Jaramillo, J.; Gomperts, R.; Stratmann, R. E.; Yazyev, O.; Austin, A. J.; Cammi, R.; Pomelli, C.; Ochterski, J. W.; Ayala, P. Y.; Morokuma, K.; Voth, G. A.; Salvador, P.; Dannenberg, J. J.; Zakrzewski, V. G.; Dapprich, S.; Daniels, A. D.; Strain, M. C.; Farkas, O.; Malick, D. K.; Rabuck, A. D.; Raghavachari, K.; Foresman, J. B.; Ortiz, J. V.; Cui, Q.; Baboul, A. G.; Clifford, S.; Cioslowski, J.; Stefanov, B. B.; Liu, G.; Liashenko, A.; Piskorz, P.; Komaromi, I.; Martin, R. L.; Fox, D. J.; Keith, T.; Al-Laham, M. A.; Peng, C. Y.; Nanayakkara, A.; Challacombe, M.; Gill, P. M. W.; Johnson, B.; Chen, W.; Wong, M. W.; Gonzalez, C.; Pople, J. A. *Gaussian 03*, revision A.3; Gaussian, Inc.: Pittsburgh, PA, 2003.
(23) Gasteiger, J.; Marsili, M. *Tetrahedron* **1980**, *36*, 3219.
(24) La Motta, C.; Sartini, S.; Mugnaini, L.; Simorini, F.; Taliani, S.; Salerno, S.; Marini, A. M.; Da Settimo, F.; Lavecchia, A.; Novellino, E.; Cantore, M.; Failli, P.; Ciuffi, M. *J. Med. Chem.* **2007**, *50*, 4917.
(25) Da Settimo, F.; Primofiore, G.; Da Settimo, A.; La Motta, C.; Taliani, S.; Simorini, F.; Novellino, E.; Greco, G.; Lavecchia, A.; Boldrini, E. *J. Med. Chem.* **2001**, *44*, 4359.
(26) Morris, G. M.; Goodsell, D. S.; Halliday, R. S.; Huey, R.; Hart, W. E.; Belew, R. K.; Olson, A. J. *J. Comput. Chem.* **1998**, *19*, 1639.
(27) Berendsen, H. J. C.; Grigera, J. R.; Straatsma, T. P. *J. Phys. Chem.* **1987**, *91*, 6269.
(28) Hess, B.; Bekker, H.; Berendsen, H. J. C.; Fraaije, J. G. E. M. *J. Comput. Chem.* **1997**, *18*, 1463.
(29) Kador, P. F. *Med. Res. Rev.* **1988**, *8*, 325. Kador, P. F.; Sharpless, N. E. *Biophys. Chem.* **1978**, *8*, 81. Kador, P. F.; Sharpless, N. E. *Mol. Pharmacol.* **1983**, *24*, 521. Kador, P. F.; Kinoshita, J. H.; Sharpless, N. E. *J.Med. Chem.* **1985**, *28*, 841.

JP8033227